Geochemical Perspectives Letters

Australasian microtektites: early target-projectile interaction in large impacts on Earth

L. Folco[1,2*], M. Masotta[1,2], P. Rochette[3], M. Del Rio[1,4], G. Di Vincenzo[5]

OPEN ACCESS

https://doi.org/10.7185/geochemlet.2427

Abstract

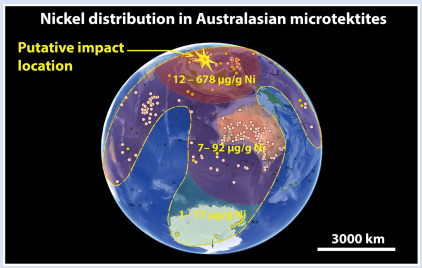

Microtektites are microscopic impact glass spherules produced by the melting and vapourisation of the Earth's crust upon hypervelocity impact of large asteroidal/cometary bodies. They are distal ejecta distributed in strewn fields extending for thousands of kilometres. We studied the geographic distribution of the impactor signature in microtektites from the Australasian strewn field using Ni contents as a proxy. Although still unidentified, geological evidence suggests an impact location in southeast Asia. Based on this assumption, the impactor signature (Ni concentrations of up to 678 µg/g; one order of magnitude higher than continental crust values) decreases with ejection distance and is not detected in the most distal microtektites from Antarctica. This evidence, coupled with trends *versus* launch distance in the concentrations of cosmogenic nuclides, volatile elements, Fe isotopes, and compositional homogeneity documented in the literature, suggests the following constraints for tektite formation models: the parent melts of the microtektites launched further away formed first, experienced the highest thermal regimes and record no impactor-target materials interaction, whereas those microtektites ejected closer formed later, experienced lower thermal regimes and record variable impactor-target materials interaction. The lack of impactor contamination in the most distal microtektites suggests that the early formed tektite/microtektite melts originated shortly before touchdown, possibly through thermal radiation in a compressed air front preceding the incoming fireball.

Received 3 April 2024 | Accepted 26 June 2024 | Published 25 July 2024

Introduction

Tektites are siliceous glass objects up to several tens of centimetres in size with splash/flanged ballistic and aerodynamic forms or blocky shapes with layered structures, *i.e.* the Muong Nong-type (*e.g.*, Glass and Simonson, 2013). Microtektites are their microscopic counterparts and typically occur in the form of spherules less than 1 mm in diameter. Tektites and microtektites are high velocity, distal impact ejecta, distributed in strewn fields extending for thousands of kilometres (*e.g.*, Glass and Simonson, 2013). They are generated by the melting and vapourisation of the Earth's continental crust during large scale (typically oblique) impacts of asteroidal/cometary bodies (Artemieva, 2002). Their volatile depleted, upper continental crust-like bulk composition derives from the involvement of large volumes of crustal materials during their formation process. As they are sourced from the top layers of the crustal targets (Ma *et al.*, 2004; Rochette *et al.*, 2018), they are a natural laboratory for investigating the chemical-physical, target-projectile interactions in large impacts. Such interactions are of critical importance for improving our understanding of the tektite/microtektite formation mechanism and of the impact melting process in general (*e.g.*, Osinski *et al.*, 2013; Goderis *et al.*, 2017).

Evidence for chemical-physical, target-projectile interactions has been recently reported in some tektites and many microtektites from the Australasian strewn field (Fig. 1; Folco *et al.*, 2023). In our previous paper we interpreted the high Ni concentrations (>100 µg/g Ni and up to 678 µg/g), *i.e.* well above the average upper continental crustal value (20 µg/g Ni; Taylor and McLennan, 1995), and relatively low Mg contents, as related to a chondritic impactor contamination of up to ~6 % by mass. We also presented several geochemical arguments to exclude the alternative explanation of this enrichment by terrestrial ultramafic contamination. In this work, we study the geographic control in the distribution of this signature in the strewn field. We focus on microtektites because, in contrast to macroscopic tektites, they 1) have a wider and more continuous distribution from southeast Asia to Antarctica, from the Indian to the Pacific oceans, and 2) they are sourced from the topmost layer of the target, based on ^{10}Be data (Rochette *et al.*, 2018) and thus the target material that experienced interaction with the projectile first. Here we show a relationship between impactor signature and ejection distance that opens new perspectives in the understanding of the target-projectile interactions, impact melting, and ejection in large scale impacts on Earth at the very contact.

1. Dipartimento di Scienze ella Terra, Università di Pisa, Via Santa Maria, 53, 56126, Pisa, Italy
2. Centro per la Integrazione della Strumentazione dell'Università di Pisa, CISUP, Lungarno Pacinotti 43/44, 56126 Pisa, Italy
3. Aix-Marseille Université, CNRS, IRD, INRAE, CEREGE, Aix en Provence, France
4. Dipartimento di Matematica e Geoscienze, Università di Trieste, Via Weiss, 2, 34128 Trieste, Italy
5. Istituto di Geoscienze e Georisorse – CNR, Via Moruzzi 1, 56124 Pisa, Italy
* Corresponding author (email: luigi.folco@unipi.it)

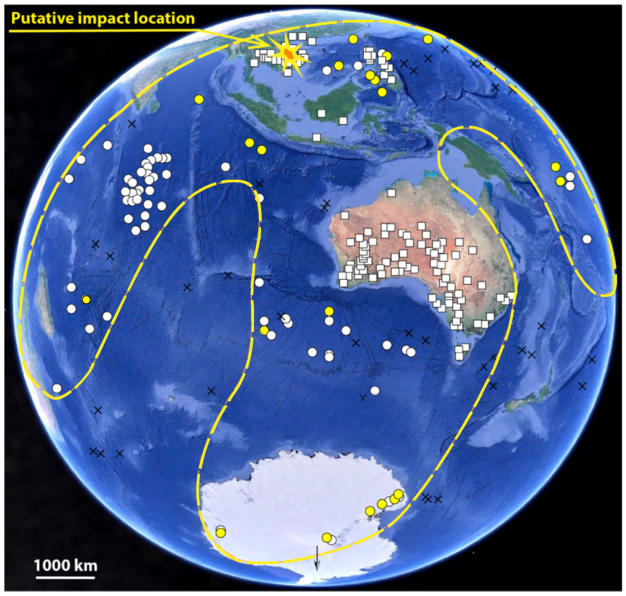

Figure 1 The Australasian tektite/microtektite strewn field (modified after Folco *et al.*, 2023). The find locations of tektites and microtektites are marked by squares and circles, respectively; the yellow circles are the locations of the microtektites studied in this work. The putative impact location in Indochina (Ma *et al.*, 2004) is arrowed. Tektites are found on land from Southeast Asia over much of Australia and Tasmania. Microtektites are found in deep sea sediments from the surrounding ocean basins, as well as on land in Antarctica, in the Transantarctic Mountains and Queen Maud Land. Black crosses are locations of deep sea sediment cores where microtektites were not found.

The Australasian Tektite/Microtektite Strewn Field

The Australasian tektite/microtektite strewn field covers ~15 % of the Earth's surface (Fig. 1) and formed ~0.8 million years ago (Jourdan *et al.*, 2019; Di Vincenzo *et al.*, 2021) through the hypervelocity impact of a chondritic body (*e.g.*, Goderis, *et al.*, 2017; Folco *et al.*, 2018, 2023). It is the youngest and the largest of the five Cenozoic strewn fields known: Australasian, Ivory Coast, Central European, Central America, and North America (Glass and Simonson, 2013; Rochette *et al.*, 2021). It is also the most elusive since its source crater has not yet been identified. However, evidence of high pressure phases in tektites (Cavosie *et al.*, 2018; Glass *et al.*, 2020; Masotta *et al.*, 2020) and other shocked ejecta (*e.g.*, Glass and Fries, 2008) indicate that they are linked to a crater forming event. Petrographic, geochemical, and isotopic trends (*e.g.*, geographic distribution of microtektite abundance, of Muong Nong type tektites and their ^{10}Be concentrations, *etc.*) point to an impact location in Indochina or the surrounding seas (*e.g.*, Ma *et al.*, 2004; Glass and Koeberl, 2006), or farther north in northwest China (Mizera, 2022). Ejecta distribution suggests a crater diameter in excess of 30 km (Glass and Koeberl, 2006). The tri-lobate outline of the strewn field defined by the distribution of microtektites (Fig. 1) resulted from down range, S-, SE- and SW-ward ballistic ejection of three main ejecta rays, according to Glass and Simonson (2013).

Geochemical studies and mineral inclusions in layered tektites from Indochina suggest a fine grained, sedimentary source rock, *e.g.*, greywacke or loess (Wasson, 1991; Glass and Koeberl, 2006). Consistently, the bulk composition of Australasian tektites and microtektites is strikingly similar to that of the upper continental crust, although depleted in volatile elements (*e.g.*, Glass *et al.*, 2004). A surface or near surface sedimentary deposit was proposed based on ^{10}Be studies (Ma *et al.*, 2004; Rochette *et al.*, 2018). The Nd model ages for both tektites and microtektites indicate source rocks with a Meso-Proterozoic crustal residence time (Blum *et al.*, 1992; Folco *et al.*, 2009; Soens *et al.*, 2021).

The Data Set

The microtektites studied in this work ($n = 144$, ~60 % of the total available from the literature), comprise those defining the high Ni/Mg trend identified by Folco *et al.* (2023) and interpreted as a mixing line joining the composition of the upper continental crust, taken as an approximation of the quartz-feldspathic target rock, and chondritic material as the impactor (Fig. 2). The database, reported in Table S-1, is a compilation of geochemical data from the literature (see references therein). The other microtektites available from the literature were not included in the selection because they define mixing trends with end member compositions yet to be identified (Folco *et al.*, 2023).

Microtektites range from 60 to 760 μm in diameter (Fig. S-1). Eighty seven microtektites are from sixteen deep sea sediment cores from the Celebs Sea, South China Sea, Philippine Sea, Sulu Sea, Indian and Pacific Oceans (Fig. 1, Table S-1). They vary widely in shape from spheroids to dumbell and tear drops. The majority are translucent and have vitreous lustre, dark-brown-green colour, and variable contents of vesicles (up to few tens of μm in diameter). Most (>90 %) contain undigested microscopic, shocked target relict grains, lechatelierite and fine compositional schlieren. Few are yellow-brown, transparent and optically homogenous. The fifty seven Antarctic microtektites are from six locations in the Transantarctic Mountains, namely, Schroeder Spur, Killer Nunatak, Miller Butte, Allan Hills, Larkman Nunatak and Mount Reymond, and one location in Queen Maud Land, Mount Widerø. In contrast to microtektites from deep sea sediments, they are transparent, pale-yellow in colour, virtually devoid of mineral inclusions and compositional schlieren, and only few (~15 %) contain a

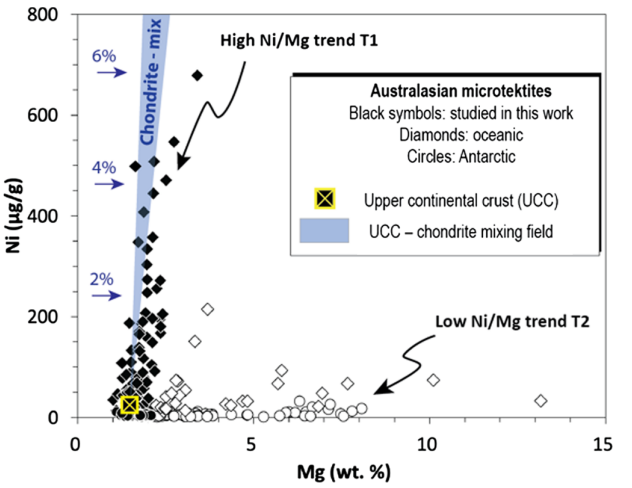

Figure 2 Nickel (μg/g) *versus* Mg (wt. %) variation diagram showing the two main Ni/Mg trends observed in Australasian microtektites ($n = 244$): the high Ni/Mg trend, T1 (black symbols; $n = 144$), and the low Ni/Mg trend, T2 (open symbols; $n = 100$) (modified after Folco *et al.*, 2023). T1 is defined by microtektites with a chondritic impactor signature up to ~6 wt. % and are distinguished from those on the T2 trend by having <2.2 Mg wt. % and >0.006 Ni/Mg for Ni <100 μg/g.

single microscopic vesicle. Except for a few with ellipsoid shapes, most are spheres.

Data Analysis

The following data analysis is based on the assumption that the still unidentified impact location is in southeast Asia, as mentioned above. Given the large extension of the Australasian strewn field, this approximation does not introduce significant bias in our discussion.

The data set shows that Ni concentrations — and thus impactor contamination — decreases, on average, with increasing distance from the putative impact location in Indochina (Fig. 3). Considering an impact location farther north in northwest China, as alternatively proposed by Mizera (2022), would not introduce significant changes. Microtektites found within 3000 km of the putative impact location ($n = 78$) show Ni contents averaging 144 µg/g and ranging 13–678 µg/g; those found at distances >3000 km and <10,000 km in the Indian and Pacific Oceans ($n = 9$) have Ni contents averaging 51 µg/g and ranging 4–120 µg/g; those found at distances >10,000 km in Antarctica ($n = 57$) have Ni contents averaging 5 µg/g and range 1–17 µg/g. The Ni contents in microtektites found at distances over 10,000 km are similar to Earth's upper continental crust values. This indicates that the most distal Antarctic microtektites yield no signature of impactor contamination, in contrast to microtektites found close to the putative impact location. The same pattern is observed for Co and Cr, taken as additional proxies for impactor contamination (Goderis *et al.*, 2017; Folco *et al.*, 2018, 2023). Cobalt and Cr decrease with launch distance from southeast Asia to Antarctica, with average and range values from 22 (4–50) to 4 (1–10) µg/g and from 145 (17–398) to 65 (25–209) µg/g, respectively (Fig. S-2).

Constraints for the Formation Model

Folco *et al.* (2010a) reported that the concentrations of volatile major elements Na and K in Australasian microtektites decreases, on average, with distance from the putative impact location: total alkalis $Na_2O + K_2O = 4.27 \pm 0.62$ wt. % and 1.25 ± 0.25 wt. % in microtektites from deep sea sediment cores within 2000 km from 17° N, 107° E and Antarctica, respectively.

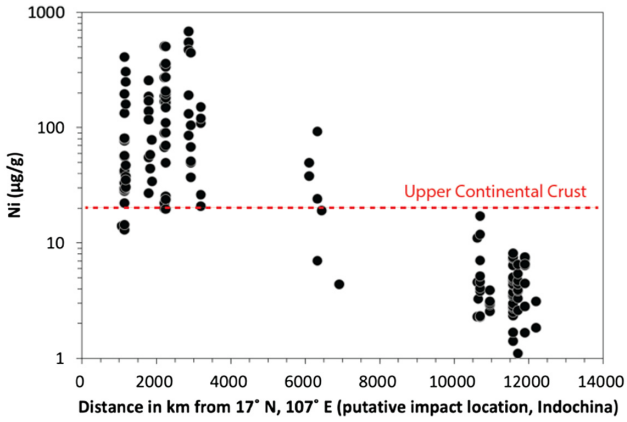

Figure 3 Nickel concentrations (µg/g) *versus* distance (km) from the putative impact location in Australasian microtektites. Geochemical data set ($n = 144$) from the literature; see Table S-1 and references therein. The putative impact location is from Ma *et al.* (2004). Nickel concentration for Earth's upper continental crust is from Taylor and McLennan (1995).

Folco *et al.* (2010b) showed that the abundance of shocked, relic grains of quartz and lechatelierite inclusions (interpreted as undigested remnants of the melting of the microtektite precursor materials), as well as compositional heterogeneities (namely, schlieren) decrease in the same fashion and become extremely low in microtektites from Antarctica. Chernonozhkin *et al.* (2021) also showed that the iron isotopic signatures covaries with the average launch distance, with the most distal Antarctic microtektites containing isotopically heavier Fe ($\delta^{56/54}Fe = 1.02 \pm 0.69$ ‰). These trends defined a relationship between increasing temperature-time regimes (regardless of the heating mechanism, *i.e.* impact, hypervelocity flight, re-entry; Folco *et al.*, 2010a; Chernonozhkin *et al.*, 2021) with greater ejection distances. Recently, Rochette *et al.* (2018) documented that ^{10}Be in microtektites increases with distance from Indochina, with average values of 125×10^6 and 184×10^6 atoms/g in oceanic and Antarctic microtektites, respectively, indicating that Antarctic microtektites were sourced from the topmost layer of the target, whereas those from lower latitudes were sourced from the underlying stratigraphic layers.

The combination of the above trends with that of the Ni *versus* distance observed in this work (Fig. 3) constitutes a set of geochemical constraints that should be taken into account in microtektite formation modelling: the greater the ejection distance, the stronger the heating they experienced, the higher the stratigraphic level of the source material in the target, and the lower the impactor contamination. This implies that the parent liquids of the most distal Australasian microtektites from Antarctica, devoid of impactor contamination and sourced from the topmost layer of the target, formed first with no chemical interaction with the (chondritic) projectile. Bearing variable impactor contamination, the parent liquids of the less distal microtektites from the seas surrounding Indochina formed (immediately) after, from the underlying stratigraphic layers, through variable yet significant mixing between target and projectile materials.

One may argue that the Ni *versus* launch distance trend is due to volatilisation since it parallels the alkali and Fe isotopes trends reported by Folco *et al.* (2010a) and Chernonozhkin *et al.* (2021), respectively. The lack of a similar trend for major and trace elements with similar condensation temperatures, *e.g.*, Mg (1340 K) and Eu (1338 K), suggests that significant Ni volatilisation (1354 K) did not take place (Fig. S-3).

Scenario

Models envision that tektites and microtektites form as an expanding spray of liquid droplets of target materials that underwent melting, partial vapourisation, high velocity ejection and fragmentation upon unloading from the high pressures generated by hypervelocity impacts of asteroidal/cometary bodies onto the Earth's crust. Models also predict accretion (to a variable extent) of condensed plume gases during atmospheric flight and, for those ejected at the highest velocities, ablation during high velocity atmospheric re-entry. All these models, either in the normal excavation flow or jetting contexts (*e.g.*, Melosh and Vickery, 1991; Artemieva, 2002; Johnson and Melosh, 2012), predict detectable amount of impactor contamination in the chemical composition of tektites/microtektites since, at this stage, around half of the projectile is involved in vapourisation and melting. This agrees with observations in Australasian microtektites found close to the impact location, but in contrast to those in the most distally deposited microtektites from Antarctica.

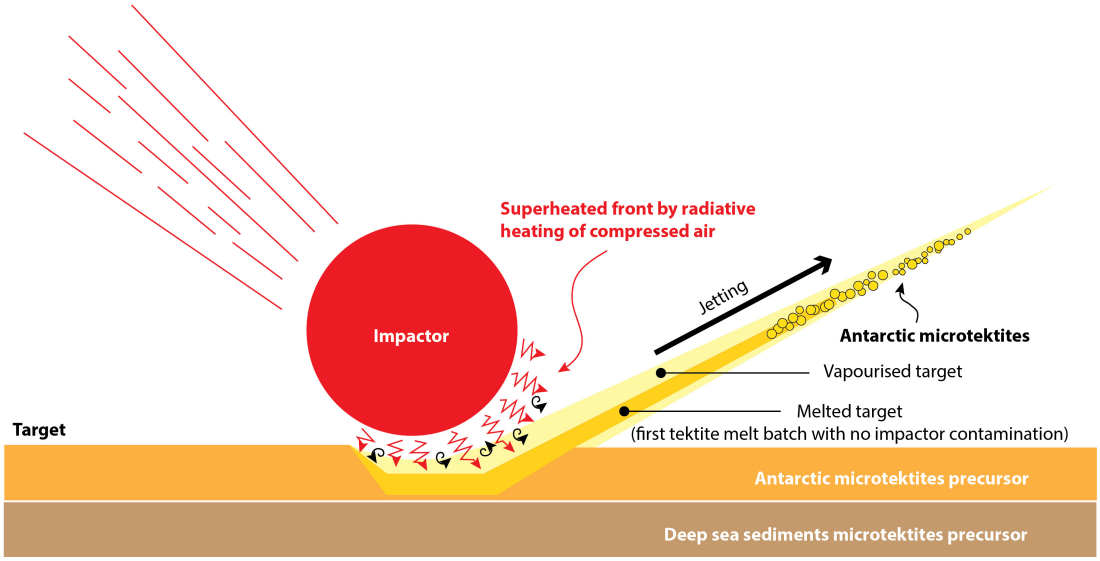

Figure 4 Schematic representation (not to scale) showing the role of radiative heating of compressed air at the front of the infalling fireball in the formation of the first tektite/microtektite melt batch. On approaching the target, melting (and vapourisation) begins just before the contact and the first tektite melt (in this work exemplified by distal microtektites from Antarctica), sourced from the topmost layer of the target, is devoid of impactor contamination. Upon subsequent contact (not shown here), compression and unloading, tektite/microtektite melts with variable impactor contamination (in this work exemplified by microtektites from deep sea sediment cores found closer to the impact location) and sourced from the underlying stratigraphic layers are produced.

The lack of impactor contamination in early formed microtektite liquids sourced from the uppermost crustal layer — here exemplified by the most distal microtektites from Antarctica — is a relevant (and apparently counterintuitive) constraint for modelling microtektite formation in large scale impacts on Earth. A plausible scenario envisions the start of the heating and melting of the very surface layers of the target — and thus the production of the first batch of tektite/microtektite melts — prior to impactor touch down, followed by squirting of the melts and compressed gas between the projectile and target into an expanding two phase jet. Sufficient heat to melt the surface layers of the target surface in excess of the tektite/microtektite liquidus of about 1400 K (*e.g.*, Masotta *et al.*, 2020) could be provided by thermal radiation in compressed air, at the front of the incoming fireball (Fig. 4). The second batch of tektite/microtektite melt, bearing variable impactor contamination, formed later when the projectile touched the ground, consistently with the occurrence of inclusions of shocked target mineral relicts (Folco *et al.*, 2010b). In this latter stage, the addition of a projectile component could occur prior to ejection when both projectile and target melts were still under elevated shock pressures, as proposed earlier by Goderis *et al.* (2017).

The proposed scenario for the formation of the first tektite/microtektite melt batch, devoid of any chemical interaction between target and projectile here exemplified by microtektites from Antarctica (Fig. 4), contrasts with the most widely accepted one which entails that heating and melting is caused by compression and adiabatic unloading during touch down of the impactor, starting soon after the contact and compression stage at the beginning of the excavation stage (*e.g.*, Melosh and Vickery, 1991; Artemieva, 2002; Osinski *et al.*, 2013). It thereby strengthens the concept that impact melting does occur in two stages, just before and after the contact of the impactor, as recently proposed by Rochette *et al.* (2024) for the formation of millimetric splash-form impact melt particles from Atacama (Atacamaites).

The model proposed here for the most distal Australasian microtektites from Antarctica (Fig. 4) envisions jetting up to enormous distances >10,000 km, assuming an impact location in the Indochina area. Di Vincenzo *et al.* (2021) showed that Antarctic microtektites contain significant amount of extraneous Ar, in striking contrast with macroscopic tektites, weakly or negligibly contaminated. Possibly, Antarctic microtektites incorporated extraneous Ar because they were enveloped within a hot gas enriched in vapourised target during ejection, while still molten droplets. Therefore, one possibility is that ejection of microtektites up to planetary distances may have occurred because Antarctic microtektites travelled within jets of gas of vapourised target (Fig. 4), perhaps assisted by atmospheric waves, similar to those recently observed in large volcanic eruptions (*e.g.*, Hunga Tonga in January 2022; Matoza *et al.*, 2022).

Acknowledgements

Transantarctic Mountains microtektite research at the University of Pisa is supported by the Italian *Programma Nazionale delle Ricerche in Antartide* (PNRA). Research on planetary materials at the University of Pisa is supported by the ASI SpaceitUP programme. The manuscript benefited from the constructive review of Steven Goderis and David Baratoux, and the careful handling of editor Romain Tartèse.

Editor: Romain Tartèse

Additional Information

Supplementary Information accompanies this letter at https://www.geochemicalperspectivesletters.org/article2427.

Cite this letter as: Folco, L., Masotta, M., Rochette, P., Del Rio, M., Di Vincenzo, G. (2024) Australasian microtektites: early target-projectile interaction in large impacts on Earth. *Geochem. Persp. Let.* 31, 22–26. https://doi.org/10.7185/geochemlet.2427

References

Artemieva, N.A. (2002) Tektite Origin in Oblique Impacts: Numerical Modeling of the Initial Stage. In: Plado, J., Pesonen, L.J. (Eds.) *Impacts in Precambrian Shields. Impact Studies*. Springer, Berlin, 257–276. https://doi.org/10.1007/978-3-662-05010-1_10

Blum, J.D., Papanastassiou, D.A., Koeberl., C., Wasserburg, G.J. (1992) Neodymium and strontium isotopic study of Australasian tektites: New constraints on the provenance and age of target materials. *Geochimica et Cosmochimica Acta* 56, 483–492. https://doi.org/10.1016/0016-7037(92)90146-A

Cavosie, A.J., Timms, N.E., Erickson, T.M., Koeberl, C. (2018) New clues from Earth's most elusive impact crater: Evidence of reidite in Australasian tektites from Thailand. *Geology* 46, 203–206. https://doi.org/10.1130/G39711.1

Chernonozhkin, S.M., González de Vega, C., Artemieva, N., Soens, B., Belza, J., Bolea-Fernandez, E., Van Ginneken, M., Glass, B.P., Folco, L., Genge, M.J., Claeys, Ph., Vanhaecke, F., Goderis, S. (2021) Isotopic evolution of planetary crusts by hypervelocity impacts evidenced by Fe in microtektites. *Nature Communications* 12, 5646. https://doi.org/10.1038/s41467-021-25819-6

Di Vincenzo, G., Folco, L., Suttle, M.D., Brase, L., Harvey, R.P. (2021) Multi-collector $^{40}Ar/^{39}Ar$ dating of microtektites from Transantarctic Mountains (Antarctica): A definitive link with the Australasian tektite/microtektite strewn field. *Geochimica et Cosmochimica Acta* 298, 112–130, https://doi.org/10.1016/j.gca.2021.01.046

Folco, L., D'Orazio, M., Tiepolo, M., Tonarini, S., Ottolini, L., Perchiazzi, N., Rochette, P., Glass, B.P. (2009) Transantarctic Mountain microtektites: Geochemical affinity with Australasian microtektites. *Geochimica et Cosmochimica Acta* 73, 3694–3722. https://doi.org/10.1016/j.gca.2009.03.021

Folco, L., Glass, B.P., D'Orazio, M., Rochette, P. (2010a) A common volatilization trend in Transantarctic Mountain and Australasian microtektites: Implications for their formation model and parent crater location. *Earth and Planetary Science Letters* 293, 135–139. https://doi.org/10.1016/j.epsl.2010.02.037

Folco, L., Perchiazzi, N., D'Orazio, M., Frezzotti, M.L., Glass, B.P., Rochette, P. (2010b) Shocked quartz and other mineral inclusions in Australasian microtektites. *Geology* 38, 211–214. https://doi.org/10.1130/G30512.1

Folco, L., Glass, B.P., D'Orazio, M., Rochette, P. (2018) Australasian microtektites: Impactor identification using Cr, Co and Ni ratios. *Geochimica et Cosmochimica Acta* 222, 550–568. https://doi.org/10.1016/j.gca.2017.11.017

Folco, L., Rochette, P., D'Orazio, M., Masotta, M. (2023) The chondritic impactor origin of the Ni-rich component in Australasian tektites and microtektites. *Geochimica et Cosmochimica Acta* 360, 231–240. https://doi.org/10.1016/j.gca.2023.09.018

Glass, B.P., Fries, M. (2008) Micro-Raman spectroscopic study of fine-grained, shock-metamorphosed rock fragments from the Australasian microtektite layer. *Meteoritics & Planetary Science* 43, 1487–1496. https://doi.org/10.1111/j.1945-5100.2008.tb01023.x

Glass, B.P., Koeberl, C. (2006) Australasian microtektites and associated impact ejecta in the South China Sea and the Middle Pleistocene supereruption of Toba. *Meteoritics & Planetary Science* 41, 305–326. https://doi.org/10.1111/j.1945-5100.2006.tb00211.x

Glass, B.P., Simonson, B.M. (2013) *Distal Impact Ejecta Layers: A Record of Large Impacts in Sedimentary Deposits*. Springer Berlin, Heidelberg. https://doi.org/10.1007/978-3-540-88262-6

Glass, B.P., Huber, H., Koeberl, C. (2004) Geochemistry of Cenozoic microtektites and clinopyroxene-bearing spherules. *Geochimica et Cosmochimica Acta* 68, 3971–4006. https://doi.org/10.1016/j.gca.2004.02.026

Glass, B.P., Folco, L., Masotta, M., Campanale, F. (2020) Coesite in a Muong Nong-type tektite from Muong Phin, Laos: Description, formation, and survival. *Meteoritics & Planetary Science* 55, 253–273. https://doi.org/10.1111/maps.13433

Goderis, S., Tagle, R., Fritz, J., Bartoschewitz, R., Artemieva, N. (2017) On the nature of the Ni-rich component in splash-form Australasian tektites. *Geochimica et Cosmochimica Acta* 217, 28–50. https://doi.org/10.1016/j.gca.2017.08.013

Johnson, B.C., Melosh, H.J. (2012) Formation of spherules in impact produced vapor plumes. *Icarus* 217, 416–430. https://doi.org/10.1016/j.icarus.2011.11.020

Jourdan, F., Nomade, S., Wingate, M.T.D., Eroglu, E., Deino, A. (2019) Ultraprecise age and formation temperature of the Australasian tektites constrained by $^{40}Ar/^{39}Ar$ analyses. *Meteoritics & Planetary Science* 54, 2573–2591. https://doi.org/10.1111/maps.13305

Ma, P., Aggrey, K., Tonzola, C., Schnabel, C., de Nicola, P., Herzog, G.F., Wasson, J.T., Glass, B.P., Brown, L., Tera, F., Middleton, R., Klein, J. (2004) Beryllium-10 in Australasian tektites: Constraints on the location of the source crater. *Geochimica et Cosmochimica Acta* 68, 3883–3896. https://doi.org/10.1016/j.gca.2004.03.026

Masotta, M., Peres, S., Folco, L., Mancini, L., Rochette, P., Glass, B.P., Campanale, F., Gueninchault, N., Radica, F., Singsoupho, S., Navarro, E. (2020) 3D X-ray tomographic analysis reveals how coesite is preserved in Muong Nong-type tektites. *Scientific Reports* 10, 20608. https://doi.org/10.1038/s41598-020-76727-6

Matoza, R.S., Fee, D., Assink, J.D., Iezzi, A.M., Green, D.N., *et al.* (2022) Atmospheric waves and global seismoacoustic observations of the January 2022 Hunga eruption, Tonga. *Science* 377, 95–100. https://doi.org/10.1126/science.abo7063

Melosh, H.J., Vickery, A.M. (1991) Melt droplet formation in energetic impact events. *Nature* 350, 494–497. https://doi.org/10.1038/350494a0

Mizera, J. (2022) Quest for the Australasian impact crater: Failings of the candidate location at the Bolaven Plateau, Southern Laos. *Meteoritics & Planetary Science* 57, 1973–1986. https://doi.org/10.1111/maps.13912

Osinski, G.R., Grieve, R.A.F., Marion, C., Chanu, A. (2013) Impact melting. In: Osinski, G.R., Pierazzo, E. (Eds.) *Impact Cratering: Processes and Products*. Wiley-Blackwell, Oxford, 125–145. https://doi.org/10.1002/9781118447307.ch9

Rochette, P., Braucher, R., Folco, L., Horng, C.S., Aumaître, G., Bourlès, D.L., Keddadouche, K. (2018) ^{10}Be in Australasian microtektites compared to tektites: Size and geographic controls. *Geology* 46, 803–806. https://doi.org/10.1130/G45038.1

Rochette, P., Beck, P., Bizzarro, M., Braucher, R., Cornec, J., Debaille, V., Devouard, B., Gattacceca, J., Jourdan, F., Moustard, F., Moynier, F., Nomade, S., Reynard, B. (2021) Impact glasses from Belize represent tektites from the Pleistocene Pantasma impact crater in Nicaragua. *Communications Earth & Environment* 2, 94. https://doi.org/10.1038/s43247-021-00155-1

Rochette, P., Di Vincenzo, G., Gattacceca, J., Barrat, J.A., Devouard, B., Folco, L., Musolino, A., Quesnel, Y. (2024) A two stage impact melting process in an impact glass strewn field from the Atacama Desert. *Geochemical Perspectives Letters* 30, 28–33. https://doi.org/10.7185/geochemlet.2418

Soens, B., van Ginneken, M., Chernonozhkin, S., Slotte, N., Debaille, V., Vanhaecke, F., Terryn, H., Claeys, P., Goderis, S. (2021) Australasian microtektites across the Antarctic continent: Evidence from the Sør Rondane Mountain range (East Antarctica). *Geoscience Frontiers* 12, 101153. https://doi.org/10.1016/j.gsf.2021.101153

Taylor, S.R, McLennan, S.M. (1995) The geochemical evolution of the continental crust. *Reviews of Geophysics* 33, 241–265. https://doi.org/10.1029/95RG00262

Wasson, J.T. (1991) Layered tektites: a multiple impact origin for the Australasian tektites. *Earth and Planetary Science Letters* 102, 95–109. https://doi.org/10.1016/0012-821X(91)90001-X

Geochemical Perspectives Letters

Australasian microtektites: early target-projectile interaction in large impacts on Earth

L. Folco, M. Masotta, P. Rochette, M. Del Rio, G. Di Vincenzo

Supplementary Information

The Supplementary Information includes:

- Table S-1
- Figures S-1 to S-3
- Supplementary Information References

Supplementary Table

Table S-1 Major element (oxides, wt. %) and trace element (Ni, Co, Cr, and Eu) contents of Australasian microtektites used in this work. Microtektites are listed according to site of provenance, in alphabetical order.

Table S-1 is available for download (.xlsx) from the online version of this article at http://doi.org/10.7185/geochemlet.2427.

Supplementary Figures

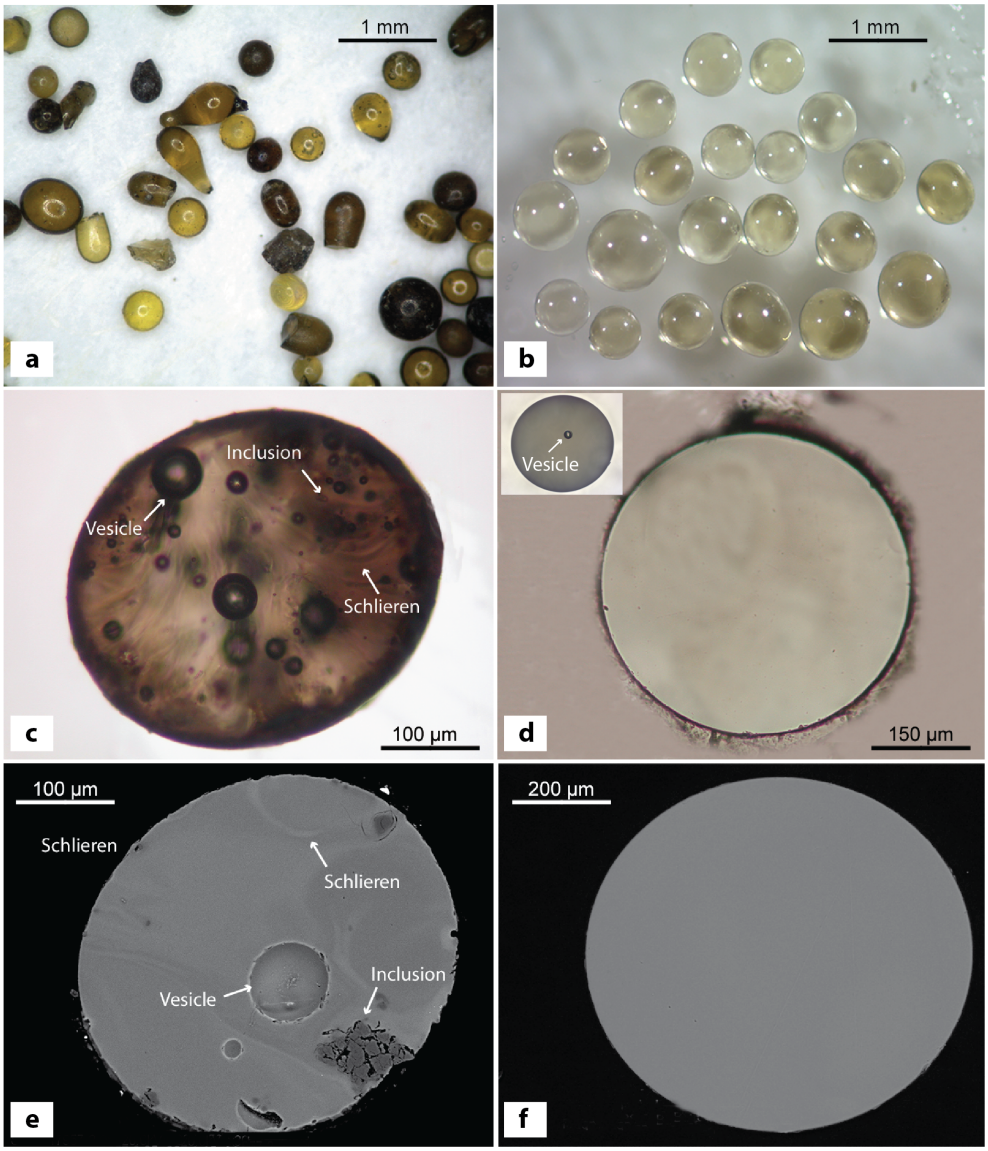

Figure S-1 Main petrographic features of the microtektites studied in this work. **(a)** A batch of microtektites from deep-sea sediments (stereomicrograph). **(b)** Stereomicrograph of a set of microtektites from the Transantarctic Mountains. **(c)** Micrograph of a sectioned microtektite from deep sea sediments found within 3000 km from the putative impact location in Indochina. **(d)** Micrograph of a sectioned microtektite from the Transantarctic Mountains. Inset: a 25 µm diameter vesicle in a sectioned microtektite from the Transantarctic Mountains 430 µm across. For the few lechatelierite inclusions observed in the Transantarctic Mountains microtektites, see Figure 4c in Folco *et al.* (2009). **(e)** Back scattered electron image of a sectioned microtektite from deep sea sediments found within 3000 km from the putative impact location in Indochina. **(f)** Backscattered electron image of a sectioned microtektite from the Transantarctic Mountains. See main text for details.

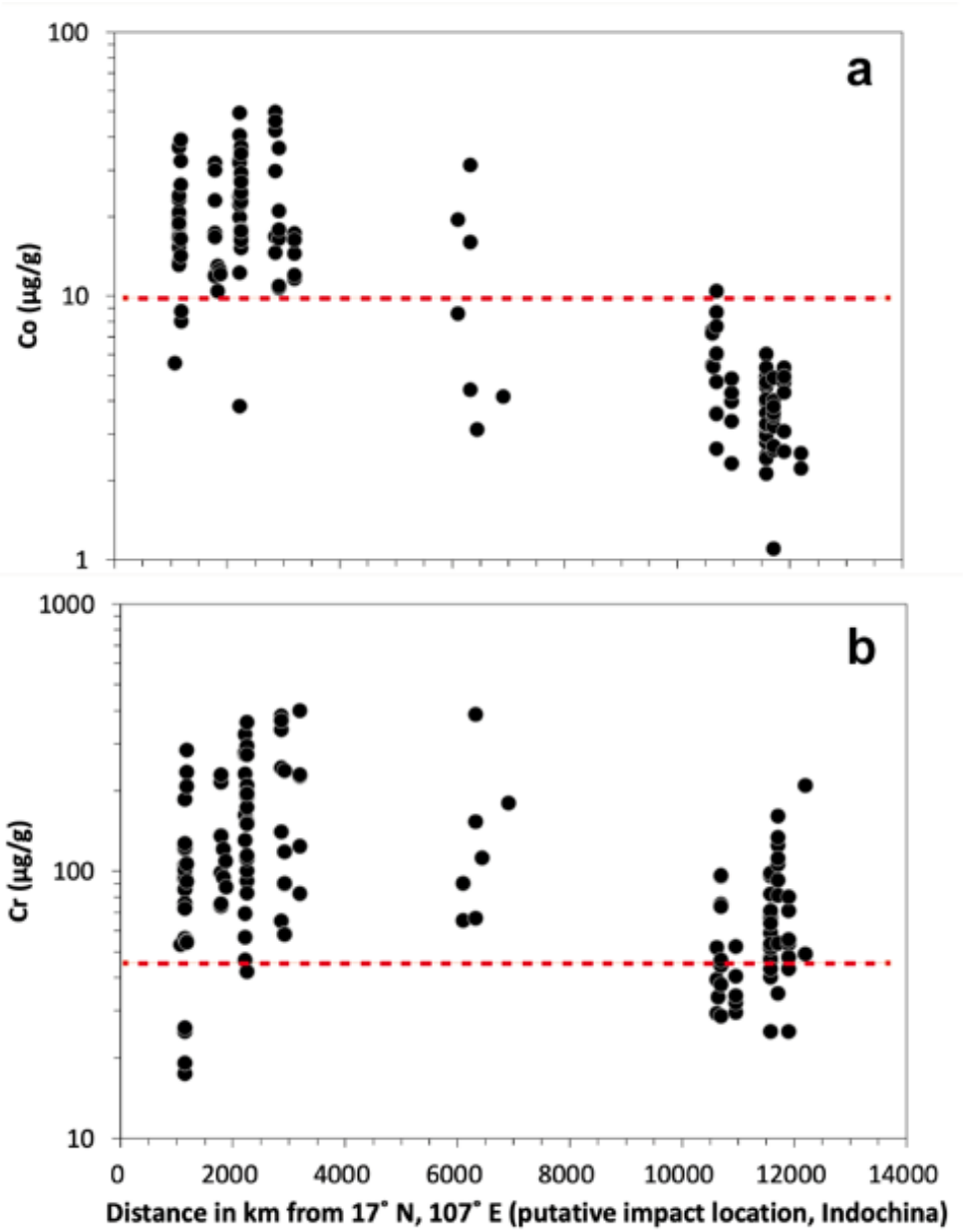

Figure S-2 **(a)** Cobalt and **(b)** Cr concentrations (µg/g) versus distance (km) from the putative impact location in Australasian microtektites. Geochemical data set (n = 144) from Brase *et al.* (2021), Folco *et al.* (2009, 2016, 2018), Glass *et al.* (2004), Glass and Koeberl (2006), Soens *et al.* (2021) and Chernonozhkin *et al.* (2021); see **Table S-1**. The putative impact location is from Ma *et al.* (2004). Cobalt and Cr concentrations for Earth's upper continental crust are from Taylor and McLennan (1995).

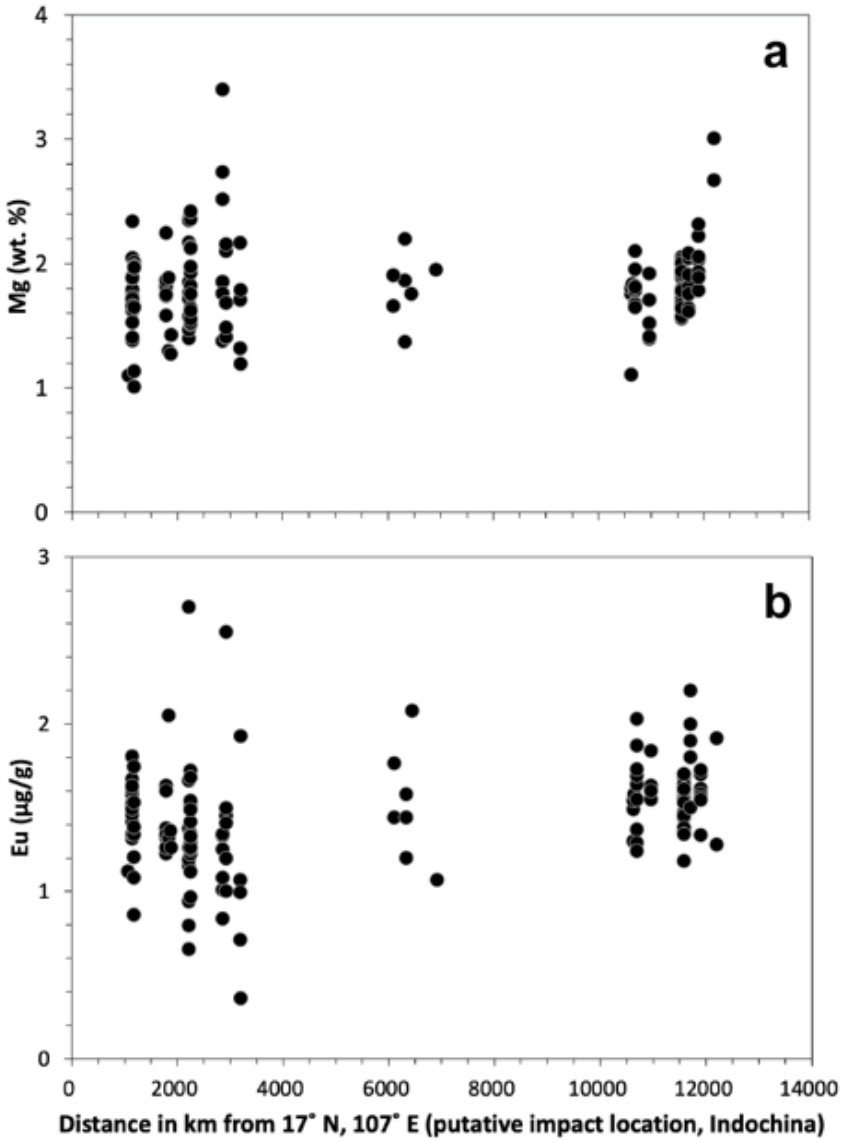

Figure S-3 **(a)** Magnesium and **(b)** Eu concentrations (µg/g) versus distance (km) from the putative impact location in Australasian microtektites. Geochemical data set (n = 144) from Brase *et al.* (2021), Folco *et al.* (2009, 2016, 2018), Glass *et al.* (2004), Glass and Koeberl (2006), Soens *et al.* (2021) and Chernonozhkin *et al.* (2021); see **Table S-1**. The putative impact location is from Ma *et al.* (2004).

Supplementary Information References

Brase, L.E., Harvey, R., Folco, L., Suttle, M.D., McIntosh, E.C., Day, J.M.D., Corrigan, C.M. (2021) Microtektites and glassy micrometeorites from new sites in the Transantarctic Mountains, Antarctica. *Meteoritics & Planetary Science* 56, 829–843. https://doi.org/10.1111/maps.13634

Chernonozhkin, S.M., González de Vega, C., Artemieva, N., Soens, B., Belza, J., Bolea-Fernandez, E., Van Ginneken, M., Glass, B.P., Folco, L., Genge, M.J., Claeys, Ph., Vanhaecke, F., Goderis, S. (2021) Isotopic evolution of planetary crusts by hypervelocity impacts evidenced by Fe in microtektites. *Nature Communications* 12, 5646. https://doi.org/10.1038/s41467-021-25819-6

Folco, L., D'Orazio, M., Tiepolo, M., Tonarini, S., Ottolini, L., Perchiazzi, N., Rochette, P., Glass, B.P. (2009) Transantarctic Mountain microtektites: Geochemical affinity with Australasian microtektites. *Geochimica et Cosmochimica Acta* 73, 3694–3722. https://doi.org/10.1016/j.gca.2009.03.021

Folco, L., D'Orazio, M., Gemelli, M., Rochette, P. (2016) Stretching out the Australasian microtektite strewn field in Victoria Land Transantarctic Mountains. *Polar Science* 10, 147–159. https://doi.org/10.1016/j.polar.2016.02.004

Folco, L., Glass, B.P., D'Orazio, M., Rochette, P. (2018) Australasian microtektites: Impactor identification using Cr, Co and Ni ratios. *Geochimica et Cosmochimica Acta* 222, 550–568. https://doi.org/10.1016/j.gca.2017.11.017

Glass, B.P., Koeberl, C. (2006) Australasian microtektites and associated impact ejecta in the South China Sea and the Middle Pleistocene supereruption of Toba. *Meteoritics & Planetary Science* 41, 305–326. https://doi.org/10.1111/j.1945-5100.2006.tb00211.x

Glass, B.P., Huber, H., Koeberl, C. (2004) Geochemistry of Cenozoic microtektites and clinopyroxene-bearing spherules. *Geochimica et Cosmochimica Acta* 68, 3971–4006. https://doi.org/10.1016/j.gca.2004.02.026

Ma, P., Aggrey, K., Tonzola, C., Schnabel, C., de Nicola, P., Herzog, G.F., Wasson, J.T., Glass, B.P., Brown, L., Tera, F., Middleton, R., Klein, J. (2004) Beryllium-10 in Australasian tektites: Constraints on the location of the source crater. *Geochimica et Cosmochimica Acta* 68, 3883–3896. https://doi.org/10.1016/j.gca.2004.03.026

Soens, B., van Ginneken, M., Chernonozhkin, S., Slotte, N., Debaille, V., Vanhaecke, F., Terryn, H., Claeys, P., Goderis, S. (2021) Australasian microtektites across the Antarctic continent: Evidence from the Sør Rondane Mountain range (East Antarctica). *Geoscience Frontiers* 12, 101153. https://doi.org/10.1016/j.gsf.2021.101153

Taylor, S.R, McLennan, S.M. (1995) The geochemical evolution of the continental crust. *Reviews of Geophysics* 33, 241–265. https://doi.org/10.1029/95RG00262